TEMPERATURE FIELD IN THE ROTOR OF A THERMALLY STRESSED ELECTRICAL MACHINE

V. V. Bandurin, P. M Kolesnikov,
O. N. Kostikov, I. P. Miroshnik,
and F. F. Rimek

UDC 536.24

The temperature field in the rotor of a thermally stressed high-speed electrical machine is investigated. The problem is solved on a computer by the grid method. Results of computation of the temperature field in the rotor for different conditions of cooling are presented.

The study of the exact distribution of the temperature field in an electrical machine is of considerable interest, because the temperature level determines the service life and the reliability of operation of the machine. A predetermination of the temperature field is especially important for the rotors of thermally stressed high-speed machines, in which a direct measurement of temperatures is very difficult and sometimes impossible from considerations of strength.

There are several known methods of computing temperature in an electrical machine.

1) The method of equivalent thermal conversion circuits is only approximate; it can only yield the average temperatures of the elements of the electrical machine [1, 2].

2) The electrical modeling of heat propagation enables one to determine the temperature field, but it requires the construction of special modeling (analog) equipment [3, 4].

3) Analytical methods of determining the temperature field have the disadvantage that an analytical solution can only be obtained for linear problems with boundary conditions such as will permit the separation of variables [5, 6], and for a small number of problems of nonlinear heat conduction [6, 7].

4) Numerical methods of computing the temperature field offer good prospects of obtaining complete information about the heat propagation in a short time.

The complete determination of the temperature field in an electrical machine in different operating modes and for different methods of cooling is a very difficult problem, since in general it is necessary to solve three-dimensional nonlinear heat-propagation equations together with nonlinear hydrodynamic equations and the equations of electromagnetic processes in the electrical machine. Therefore a number of assumptions are made in order to simplify the problem; as the information builds up these assumptions have to be refined.

In the present work, the temperature field in the transverse cross section of an electrical machine is investigated under steady-state operating and cooling conditions. Heat generation due to losses is characterized by values obtained experimentally. The heat distribution in the cooling liquid is not taken into consideration, and the heat elimination is described in terms of the average temperature of the liquid and the average heat-transfer coefficient. The thermophysical properties of the materials are assumed constant.

The construction of the machine under consideration is shown in Fig. 1, where the main details of the rotor and the stator in the transverse section of the machine are depicted. In view of symmetry, only one sector of the machine is shown.

Institute of Heat and Mass Transfer of the Academy of Sciences of the Belorussian SSR, Minsk. Institute of Electrodynamics and Institute of Cybernetics of the Academy of Sciences of the Ukrainian SSR, Kiev. Aviation Institute, Khar'kov. Translated from Inzhenerno-Fizicheskii Zhurnal, Vol. 17, No. 3, pp. 491-498, September, 1969. Original article submitted October 22, 1968.

© *1972 Consultants Bureau, a division of Plenum Publishing Corporation, 227 West 17th Street, New York, N. Y. 10011. All rights reserved. This article cannot be reproduced for any purpose whatsoever without permission of the publisher. A copy of this article is available from the publisher for $15.00.*

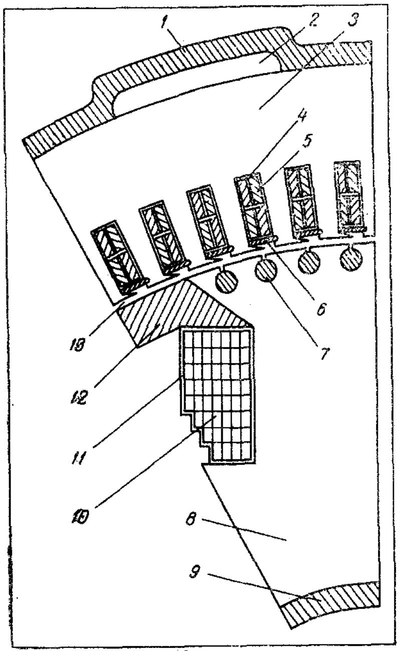

Fig. 1

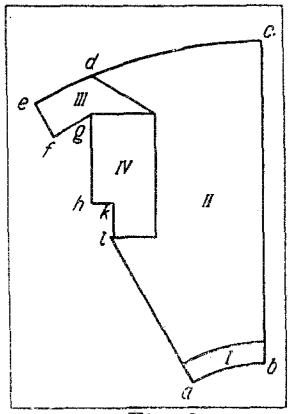

Fig. 2

Fig. 1. A sector of the transverse section of the electrical machine: 1) frame; 2) cooling channel for the stator; 3) stator core; 4) groove insulation; 5) stator winding; 6) groove wedge; 7) damper rods; 8) rotor core; 9) rotor shaft; 10) excitation coil; 11) frame insulation of the excitation coil; 12) interpole wedge; 13) gap between the rotor and stator.

Fig. 2. Computational model of a rotor.

The stator is cooled by a liquid flowing in the channels between the frame of the machine and the laminated core. The rotor is cooled by pumping the liquid into its hollow shaft and the channels between the excitation coils; the interpole wedge is also cooled in this process.

The temperature field is only determined in the rotor of the electrical machine, and the thermal coupling with the stator is taken into consideration by specifying the thermal flux between the rotor and the stator. The complete problem of determining the temperature field over the entire sector of the machine will be investigated later. Even the transverse section of the rotor alone has very complex boundaries and includes many diverse elements; the simpler model, shown in Fig. 2, was therefore chosen for the computation.

The simplifications introduced are evident from a comparison of Figs. 1 and 2: the damper winding rods are excluded from the discussion, a simpler geometry of the excitation coil is used, and its frame insulation is omitted.

These simplifications are expedient in working out the computational program; they also permit a qualitative comparison of the obtained results with known results [8].

Heat evolution of density q_{IV} occurs in the region of the coil IV only. In the remaining regions I, II, and III there is no heat evolution. The surface losses and the losses in the damper winding are given in the form of a thermal flux into the region across its boundary, computed from the thermal conversion circuit and the heat-balance equation.

In region IV of the excitation coils the heat propagation is described by Poisson's equation

$$\frac{\partial^2 T_{IV}}{\partial x^2} + \frac{\partial^2 T_{IV}}{\partial y^2} = -\frac{q_{IV}}{\lambda_{IV}},$$

where T_{IV} is the temperature in the region of the coil; λ_{IV} is the thermal conductivity of the coil; and x, y are the coordinates.

In regions I, II, and III the heat distribution is described by the Laplace equation

$$\frac{\partial^2 T_i}{\partial x^2} + \frac{\partial^2 T_i}{\partial y^2} = 0,$$

where i = I, II, and III is the index of the corresponding region.

In order to solve the equation it is necessary to specify the boundary conditions on all the boundaries of the model and also the coupling conditions between the regions. These are obtained from the requirement that the temperatures and thermal fluxes at the boundaries of different media should be continuous.

At the boundaries b−c, e−f, $l-a$ the condition

$$\frac{\partial T}{\partial n} = 0.$$

is satisfied by virtue of the thermal symmetry. The experimentally obtained value is specified at the boundary a−b.

There is a flow of heat between the stator and the rotor along the entire boundary c−d−e; the surface losses and losses in the damper have to be taken into consideration along c−d.

At the boundary a−b the boundary condition has the form

$$-\lambda_{\mathrm{I}} \frac{\partial T_{\mathrm{I}}}{\partial n} = P_{ab},$$

where λ_{I} is the coefficient of thermal conductivity of region I; P_{ab} is the specific thermal flux across the boundary a−b; n is the normal to the boundary. The condition at the boundary c−d is

$$-\lambda_{\mathrm{II}} \frac{\partial T_{\mathrm{II}}}{\partial n} = -P_{cd};$$

at the boundary e−d

$$-\lambda_{\mathrm{III}} \frac{\partial T_{\mathrm{III}}}{\partial n} = -P_{ed};$$

at the boundary f−g

$$-\lambda_{\mathrm{III}} \frac{\partial T_{\mathrm{III}}}{\partial n} = P_{fg};$$

at the boundary g−h−k−l

$$-\lambda_{\mathrm{IV}} \frac{\partial T_{\mathrm{IV}}}{\partial n} P_{ghkl},$$

where λ_i is the thermal conductivity of the corresponding region; and P is the flux across unit surface of the region.

The Laplace and Poisson equations cannot be solved analytically, since the complexity of the boundary conditions does not permit separation of the variables.

In order to secure a numerical solution of the equations of the temperature field with boundary conditions of the mixed type, it is necessary to specify the values of the constants characterizing the heat-conducting properties of the materials used, the numerical values of the thermal fluxes, or the values of the temperatures at the outer boundaries of the model.

For region IV the thermal conductivity λ_{IV} is taken as the resultant value of the thermal conductivity of the whole coil, which is regarded as being rectangular wire. The thermal conductivity coefficients for regions I, II, and III are chosen in accordance with the average temperatures in these regions.

In all the computations the coefficients of thermal conductivity had the following values:

$$\lambda_{\mathrm{I}} = 9.4;\ \lambda_{\mathrm{II}} = 20;$$
$$\lambda_{\mathrm{III}} = 168;\ \lambda_{\mathrm{IV}} = 2.76\ \mathrm{W/m \cdot {}^\circ K}.$$

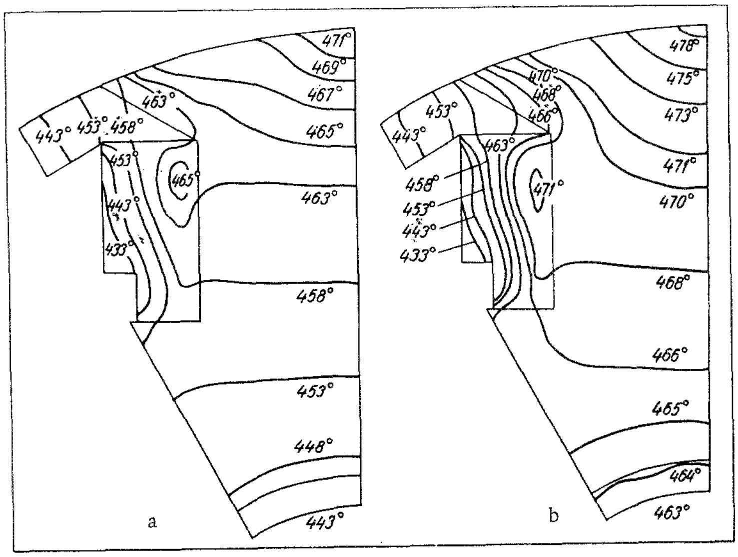

Fig. 3. Temperature field of the rotor for T_{ab} = 463°K (b) and and T_{ab} = 443°K (a).

The equivalent thermal conversion circuit of the entire electrical machine was solved for different operating conditions and different methods of cooling in order to determine the thermal fluxes in the rotor.

The temperatures at some of the outer boundaries computed in this way were compared with experimentally-determined temperatures and taken as a basis for the numerical computation.

All the necessary data for carrying out the numerical computation of the temperature field in the transverse section of the electrical machine were obtained in this way.

The heat-transfer equation with mixed-type boundary conditions and with selected values of the thermophysical parameters of the materials and thermal fluxes was solved by the grid method. For this purpose the differential equations and the boundary conditions were replaced by finite-difference equations and conditions. All the regions of the computing model were covered with a square grid of identical step h; the value of the step was varied in estimating the accuracy of the computation.

The Laplace equation has the form

$$T_{i-1,j} + T_{i,j-1} + T_{i+1,j} + T_{i,j+1} - 4\,T_{i,j} = 0,$$

where i and j are the indices of the grid point.

In the grid model, Poisson's equation is written in the form

$$T_{i-1,j} + T_{i,j-1} + T_{i+1,j} + T_{i,j+1} - 4\,T_{i,j} = -h^2\,\frac{q_{\mathrm{IV}}}{\lambda_{\mathrm{IV}}}.$$

It is well known that in this case the error of the approximation is $O(h^2)$.

For points at a distance smaller than h/2 from the lines separating two regions the difference analog of the coupling condition is taken.

For example, in the case of points at a distance of less than a half step from the line separating regions I and II this condition has the form

$$T_{i,j} = \frac{1}{1 + C_{12}}\left[\frac{x_i}{y_j}\,(T_{i+1,j+1} + C_{12}T_{i-1,j-1}) + \left(1 - \frac{x_i}{y_j}\right)(T_{i,j+1} + C_{12}T_{i,j-1})\right],$$

where $C_{12} = \lambda_I/\lambda_{II}$. For points at distances of less than a half step from the line separating regions II and III the coupling condition has the form

$$T_{ij} = \frac{1}{2(1 + C_{23})}\,[T_{i+1,j-1} + T_{i,j-1} + C_{23}(T_{i,j+1} + T_{i-1,j+1})],$$

where $C_{23} = \lambda_{II}/\lambda_{III}$.

The derivatives along the inward normal are approximated in the boundary conditions in a similar way. At the boundary c–d the difference analog of the boundary condition is the following:

$$T_{ij}=\frac{x_i}{y_j}(T_{i-1,j-1}-T_{i,j-1})+T_{i,j-1}+\frac{hP_{cd}}{\lambda_{II}}\sqrt{1+\left(\frac{x_i}{y_j}\right)^2};$$

at the boundary d–e

$$T_{ij}=\frac{x_i}{y_j}(T_{i-1,j-1}-T_{i,j-1})+T_{i,j-1}+\frac{hP_{cd}}{\lambda_{III}}\sqrt{1+\left(\frac{x_i}{y_j}\right)^2};$$

at the boundary e–f, $l-a$

$$T_{ij}=\frac{\sqrt{3}}{3}(T_{i-1,j+1}-T_{i-1,j})+T_{i-1,j};$$

at the boundary f–g

$$T_{ij}=\frac{\sqrt{3}}{3}(T_{i+1,j+1}-T_{i,j+1})+T_{i,j+1}-\frac{2hP_{fg}}{\sqrt{3}\lambda_{III}};$$

at the boundary g–h, k–l

$$T_{ij}=T_{i-1,j}-\frac{hP_{ghkl}}{\lambda_{IV}};$$

at the boundary h–k

$$T_{ij}=T_{i,j+1}-\frac{hP_{ghkl}}{\lambda_{IV}};$$

at the boundary b–c

$$T_{0j}=T_{1j};$$

at the boundary a–b

$$T_{ij}=\frac{x_i}{y_j}(T_{i+1,j-1}-T_{i,j+1})+T_{i,j+1}-\frac{hP_{ab}}{\lambda_{I}}\sqrt{1+\left(\frac{x_i}{y_j}\right)^2}.$$

As a result of the replacement of the differential equations by difference equations and the boundary conditions by difference boundary conditions a system of linear algebraic equations is obtained; the order of the system is equal to the number of nodes of the sector in which the solution is sought.

The method of block iteration (explicit scheme) is used to solve the system of linear algebraic equations.

The accuracy ε with which the computations are to be made is specified before the start of the iteration process.

In regions I, II, and III the computation was carried out according to the formula

$$T_{ij}^{(k)}=\frac{1}{4}(T_{i-1,j}^{(k)}+T_{i,j-1}^{(k)}+T_{i+1,j}^{(k-1)}+T_{i,j+1}^{(k-1)}),$$

where (k) is the number of the iteration; and (k – 1) is the number of the preceding iteration.

In region IV the computation is carried out using the formula

$$T_{ij}^{(k)}=\frac{1}{4}\left(T_{i-1,j}^{(k)}+T_{i,j-1}^{(k)}+T_{i,j+1}^{(k-1)}+T_{i+1,j}^{(k-1)}+\frac{h^2q_{IV}}{\lambda_{IV}}\right).$$

The computation ends when the condition

$$\max_{i,j}(T_{ij}^{(k)}-T_{ij}^{(k-1)})<\varepsilon$$

is satisfied.

The program is compiled in the algorithmic language "Algol-60."

The results of a numerical computation of the heat-transfer equations at 450 nodal points of the grid are presented in Fig. 3a and b. We shall now analyze these results.

The isotherms of the temperature field of the rotor are plotted in Fig. 3a for the following values of the parameters:

$$q_{IV} = 2.540 \cdot 10^6 \text{ W/m}^2 \quad P_{ab} = 1.316 \cdot 10^4 \text{ W/m}^2$$
$$P_{cd} = 2.038 \cdot 10^4 \text{ W/m}^2 \quad P_{ed} = 0.298 \cdot 10^4 \text{ W/m}^2$$
$$P_{fg} = 4.080 \cdot 10^4 \text{ W/m}^2 \quad P_{ghkl} = 2.530 \cdot 10^4 \text{ W/m}^2$$
$$T_{ab} = 463 \text{ °K}.$$

The paths of the thermal flux in the rotor may be clearly traced from the isotherms of Fig. 3a. Almost all the losses in the excitation coil pass through the surface directly washed by the liquid; a small part of the losses pass the interpole wedge, the rotor core, and the hollow shaft. The surface and damper losses are transferred to the coolant through the interpole wedge and the rotor core. The distribution of the heat flux may be qualitatively estimated from the density of the isotherms and the sections across which these thermal fluxes pass.

Figure 3b shows a temperature field corresponding to more intensive heat transfer. The thermal flux along the corresponding boundaries remains the same as before, but the temperature level is lowered due to the increase in the heat-transfer coefficient. The maximum temperature in the coil has become 464°K and its position has moved closer to the interpole wedge; this is due to a redistribution of the thermal flux.

The following conclusions may be drawn from the analysis of these computations.

The temperature fields presented in the figures give a clear picture of the distribution of the temperature field and the path along which the thermal flux travels in the rotor of a thermally stressed machine. In the absence of cooling in the gap between the rotor and the stator, the most strongly heated part of the excitation coil is that immediately adjoining the core and the interpole wedge. A clearly defined maximum of the temperature field occurs in the region of the excitation coil. The position of the point of maximum temperature changes with changing operating and cooling conditions; this is clearly seen from a comparison of Fig. 3a and b. If the rotor is also cooled in the gap between the rotor and the stator, the coil itself becomes the most thermally stressed region in the rotor, which is hazardous from the point of view of electrical insulation cost. Any intensification of the cooling of the rotor leads, of course, to a reduction in the temperature level, which is evident from Fig. 3a and b. The paths of the thermal flux lie along the normals to the isotherms and their intensity may be estimated from the density of the isotherms in separate segments of the rotor. The complete pattern of the temperature field distribution enables us to estimate the efficiency of different methods of cooling and choose the most suitable cooling conditions, which is important in the construction of electrical machines.

The fact that several regions (the insulation of the excitation coil, the regions of the damper windings (see Fig. 1)) are not represented in the model somewhat reduces the value of the computations in the sense of the completeness of the temperature-field pattern in a real machine; however, this simplified model enables us to compile a computation program, to estimate its accuracy, and to obtain temperature-field distribution patterns in qualitative agreement with the computations of [8].

The computation of one particular version of the temperature field of the rotor at 450 points in the region takes 19 min on the "M-20" computer. The program enables us to investigate different cooling conditions in machines with different constructional materials.

LITERATURE CITED

1. I. F. Filippov, Problems of Cooling of Electrical Machines [in Russian], Énergiya, Moscow–Leningrad (1964).
2. G. G. Schastlivyi, Heating of Closed Asynchronous Electric Motors [in Russian], Naukova Dumka, Kiev (1966).
3. B. A. Volynskii and V. E. Bukhman, Models for Solution of Boundary Value Problems [in Russian], Fizmatgiz, Moscow–Leningrad (1960).

4. W. Karplus, Modeling Equipment for Solution of Problems of Field Theory [Russian translation], IL, Moscow (1962).
5. G. Gotter, Heating and Cooling of Electrical Machines [in Russian], Gosénergoizdat, Moscow–Leningrad (1961).
6. A. V. Lykov, Theory of Thermal Conductivity [in Russian], Vysshaya Shkola, Moscow (1967).
7. Ya. B. Zel'dovich and Yu. P. Raizer, Physics of Shock Waves and High-Temperature Gasdynamic Phenomena [in Russian], Fizmatgiz, Moscow (1963).
8. P. Richards, Electrical Engineering (September, 1958).